THE ASTROPHYSICAL JOURNAL, 479:560–567, 1997 April 20

RADIATIVE ASSOCIATION RATES AND STRUCTURE OF RESONANCES FOR Li AND Li^+ COLLIDING WITH H AND H^+

F. A. GIANTURCO AND P. GORI GIORGI
Department of Chemistry, The University of Rome, Città Universitaria, 00185 Rome, Italy
Received 1996 May 2; accepted 1996 November 7

ABSTRACT

The radiative association rates are computed, using an entirely ab initio approach, for Li and Li^+ atoms interacting with H and H^+. The accurate potential energy curves obtained for such systems in an earlier study (Gianturco et al. 1996) are employed, and the corresponding transition moments are also used to evaluate the cross sections. The final rates are shown generally to decrease with temperature in the range from 50 to 5000 K, in close agreement with the behavior of recent calculations (Dalgarno et al. 1996). At low collision energies, all the systems considered show interesting resonant structures that can be associated to specific final states of the bound products of the reactions. The importance of these rates of formation in the lithium chemistry of the early universe is also briefly discussed.

Subject headings: atomic processes — early universe — molecular processes

1. INTRODUCTION

As the universe expanded, different atoms and molecules got formed from free nucleons and electrons, while photoionization and photodissociation processes gradually became ineffective because of the cooling of the radiation temperature. The first galaxies and stars thus formed from a gas of H and ^{4}He with trace amounts of D, ^{3}He, and ^{7}Li. In the absence of heavier elements, the radiative cooling mentioned before was controlled by the presence of that small fraction of the gas that was molecular in nature, thus indicating that molecular cooling could be taken as the chief mechanism for primordial cloud collapse (Silk 1983; Lepp & Shull 1984). Chemistry began with the appearance of the first neutral molecule H_2, soon after the production of neutral atomic hydrogen through radiative recombination of protons and electrons. The lithium chemistry, in turn, was initiated by the recombination of lithium ions through radiative recombination and mutual neutralization:

$$Li^+ + e^- \rightarrow Li + h\nu\,, \tag{1a}$$

$$Li^+ + H^- \rightarrow Li + H \tag{1b}$$

(Lepp & Shull 1984). Because of its low ionization potential, it was pointed out (Dalgarno & Lepp 1987) that lithium may remain almost fully ionized at the time of the hydrogen recombination process; therefore, the formation of molecular species that contain lithium could be started by considering the following series of radiative association processes:

$$Li + H \rightarrow LiH + h\nu\,, \tag{2a}$$

$$Li^+ + H \rightarrow LiH^+ + h\nu\,, \tag{2b}$$

$$Li + H^+ \rightarrow LiH^+ + h\nu\,. \tag{2c}$$

This means that direct knowledge of the relative cross sections of molecular formation and the corresponding rates are of paramount importance for deciding quantities such as fractional abundance of LiH with respect to the total hydrogen nuclei or the relative ratio of number densities between LiH and LiH^+. The earlier estimates turned out to be rather uncertain because of lack of knowledge of the rates for reactions (eqs. [2a]–[2c]) (Puy et al. 1993).

In the present work we make use of recently calculated, and highly accurate, potential energy curves for the title molecules (Gianturco et al. 1996) and evaluate the cross sections of all the processes in the reactions (eq. [2]) over a broad range of temperatures. The results are obtained using a fully quantum mechanical method and compare well with the recent computations, on the same systems, by Dalgarno, Kirby, & Stancil (1996). Specific features of the resonant processes at low collision energies are also examined and are found to provide indications of the possible formation of molecular excited final states for both the neutral and the ionic species.

2. THE DIRECT RADIATIVE ASSOCIATION

As is well known, the formation of diatomic bound species through direct two-body association only becomes possible if the residual energy is released radiatively through photon emission. This is usually a process with much lower probability than associative recombination via three-body collisions, whereby the residual energy is transferred during the encounter, since in the former case the time needed to emit the photon from the excited state ($\sim 10^{-8}$ s) is much longer than the interaction time between partners ($\sim 10^{-13}$ s). It becomes the only possible alternative in the medium of the postrecombination universe, where the very low number densities give rise to very low collision numbers and make three-body collisions essentially negligible.

When one views the process within the conventional Born-Oppenheimer (BO) approximation, then the relative motion of the interacting partners could either follow adiabatically the single electronic potential energy curve (PEC) of the molecular ground state or could move first along one of the electronically excited PECs of the diatom and then radiatively reach a bound state of the ground state electronic PEC. As the latter process corresponds to a vibronic transition, it usually occurs with a greater probability than the former pure rotovibrational transitions (Herzberg 1950).

The quantum form of the corresponding cross section at a given relative collision energy of the partners could be obtained by starting from the usual Einstein coefficient for spontaneous emission between bound states of a conven-

tional diatomic target, in atomic units:

$$A_{vJ,v'J'} = \frac{32}{3c^3}\,\pi^3 v^3_{vJ,v'J'}\,\frac{S_{JJ'}}{2J+1}\,M^2_{vJ,v'J'} \tag{3}$$

(Herzberg 1950), where $M_{vJ,v'J'}$ is the dipole transition moment between the relevant rotovibrational levels,

$$M_{vJ,v'J'} = \int_0^\infty \phi_{vJ}(R)\mu(R)\phi_{v'J'}(R)dR\ , \tag{4a}$$

and $S_{JJ'}$ is the result of the angular integration in equation (4a) and is usually called the Hönl-London coefficient (Schadee 1978). The simple extension of the above transition moment to a case in which the initial wave function is an energy-normalized continuum function f_{EJ} generated by the same PEC allows one to write

$$M_{EJ,v'J'} = \int_0^\infty f_{EJ}(R)\mu(R)\phi_{v'J'}(R)dR\ . \tag{4b}$$

The probability $P(J)$ that a given initial partial wave component f_{EJ} would decay by photon emission can be obtained by dividing the corresponding $A_{EJ,v'J'}$ coefficient by the flux of incoming particles. The total cross section at a given collision energy E is further given by

$$\sigma(E) = \frac{\pi}{k^2}\sum_J (2J+1)P(J) \equiv \sum_J \sigma_J(E) \tag{5}$$

(Smith 1971), where the terms in the sum on the far right-hand side correspond to the opacity contributions, $k^2 = 2\mu E$, and all quantities are in atomic units. Each of such contributions could therefore be obtained as

$$\sigma_{J,v'J'}(E) = \frac{64}{3}\,\frac{\pi^5}{c^3}\,\frac{p}{k^2}\,v^3_{Ev'J'}\,S_{JJ'}\,M^2_{EJ,v'J'}\ , \tag{6}$$

which therefore allows us to rewrite the sum of equation (5) in the following, more specific, way:

$$\sigma(E) = \sum_{J,v',J'} \sigma_{J,v'J'}(E)\ . \tag{7}$$

To obtain the corresponding rates finally requires a further integration over a Maxwellian distribution of the partner's relative velocities,

$$K(T) = \left(\frac{8}{\mu\pi}\right)^{1/2}\left(\frac{1}{k_B T}\right)^{3/2}\int_0^\infty E\sigma(E)e^{-E/k_BT}\,dE\ , \tag{8}$$

where all quantities are expressed in atomic units. The quantity p of equation (6) describes also the relative probability of the nuclei being driven by one particular PEC of the ones available in that range of energies (Herzberg 1950; Babb & Dalgarno 1995), i.e., its relative statistical weight.

The general behavior of the individual cross sections and the effect of the various PEC features at low collision energies are functions of the specific system and will therefore behave very differently depending on the particular final diatomic product that we shall consider. Generally speaking, however, one should expect they will drop off rather rapidly with collision energy since the corresponding Franck-Condon region of maximum effect from the transition moments will play a less important role as the overlap decreases at the shorter relative distances sampled at higher collision energies.

The specific results for the various systems are analyzed in detail in the following sections.

3. RECOMBINATION CROSS SECTIONS FOR LiH

We consider the dynamics of the radiative recombination process occurring along the adiabatic PECs that connect asymptotically with $Li(1s^2 2s) + H(1s)$. Within the BO approximation, they correspond to the following Σ states: $X^1\Sigma^+$ and $a^3\Sigma^+$, which pertain to the singlet and triplet spin states, respectively. The $^3\Sigma^+$ state corresponds to a repulsive potential, and it is also dipole forbidden to combine radiatively with the singlet state of the final bound molecule. The continuum initial states could therefore belong only to the $^1\Sigma^+$ curve in order to allow the transitions into its rotovibrational bound states. The spin multiplicity also assigns the value of $p = \frac{1}{4}$ in equation (6).

The allowed rotational index changes from J into J' are for $J' = J \pm 1$, and the corresponding Hönl-London factors of equation (3) are given by

$$\begin{aligned} &J' = J+1, \text{ then } S_{JJ'} = J+1\ ; \\ &J' = J-1, \text{ then } S_{JJ'} = J \end{aligned} \tag{9}$$

(Herzberg 1950). Furthermore, we need to sum over all possible J values up to $\bar{J}' + 1$ for the R branch of the transition (for which $J' = J - 1$) and up to $\bar{J}' - 1$ for the P branch of the transition (for which $J' = J + 1$). Here $\bar{J}'$ represents the largest possible value for the rotational quantum number in the final vibrational state v'. The corresponding expression for equation (6) therefore gets rewritten as follows:

$$\sigma(E) = \frac{64}{3}\,\frac{\pi^5}{c^3}\,\frac{p}{k^2}\sum_{v'=0}^{v_{\max}}\left\{\sum_{J=1}^{\bar{J}+1} v^3_{EJ,v'J-1}\,JM^2_{EJ,v'J-1} + \sum_{J=0}^{\bar{J}'-1} v^3_{EJ,v'J+1}(J+1)M^2_{EJ,v'J+1}\right\}. \tag{10}$$

One can simplify equation (10) by grouping together terms corresponding to the same photon frequency. If one disregards the energy difference between the final bound states characterized by the $|v, J+1\rangle$ and the $|v, J-1\rangle$ indices, then one obtains for equation (10) the expression given by Zygelman & Dalgarno (1990). In the present treatment, however, we have preferred to include these slight differences between frequencies implied by the differences in rotational quantum numbers of the final bound states. Therefore, we have defined a partial cross section associated to each final vibrational state v, but starting from different trajectories between continuum energy partners:

$$\sigma_v(E) = \frac{64}{3}\,\frac{\pi^5}{c^3}\,\frac{p}{k^2}\sum_{J=0}^{\bar{J}'}\{v^3_{E,vJ}[JM^2_{EJ-1,vJ} + (J+1)M^2_{EJ+1,vJ}]\}\ . \tag{11}$$

A similar expression was also given by Kheronskii & Lipovka (1993). These authors, however, did not include the multiplicity factor $(2J+1)$ within the definition of $P(J)$ in equation (5).

The partial contributions given by equation (11) are finally grouped into the expression for the total cross section at a given relative energy E, the relative collision energy of the neutral partners:

$$\sigma(E) = \sum_{v=0}^{v_{\max}} \sigma_v(E)\ . \tag{12}$$

The partial cross sections $\sigma_v(E)$ have been evaluated for 451 different collision energy values in the interval between 10^{-4} and 10 eV. The continuum wave functions were obtained by integrating radially out to relative separations of $R \sim 350a_0$. The actual results of the final integration, as a function of both energy E and final vibrational level v, are shown in Figure 1 (*top*). One can draw the following interesting points from looking at the results:

1. The partial cross sections exhibit a very marked dependence on the final vibrational state into which the molecule is formed after radiative emission. At a given relative energy, in fact, the cross sections can vary over more than 8 orders of magnitude.

2. The number of bound vibrational states found in our calculations (for $J = 0$) is of 24 levels, with $v_{max} = 23$ (Gianturco et al. 1996), and one clearly sees in the figure that several resonances are evident in the low-energy region. It is also interesting to note that the largest partial cross section appears for $v = 18$, while the partial contributions decrease in value as v increases up to 23.

3. All partial cross sections show a rather similar, at least qualitatively, energy dependence, since they all markedly decrease as the collision energy increases. This is simply due to the fact that, as the interaction time decreases, the time interval during which the photon can be emitted becomes shorter; therefore, the collisions occur into other inelastic channels of the partner's excitations rather than by photon emission followed by the recombinative event.

The very strong dependence of $\sigma_v(E)$ on the final vibrational state of the molecule being formed is due to various factors: as the index v increases, the classically allowed region of relative distances mapped by the final vibrational wave functions increases and involves R values in which the dipole function gradient becomes larger. On the other hand, the multiplicative frequency factor in equation (11) becomes smaller very rapidly, and so does the number of terms in the sum over J as fewer rotovibrational states become available at higher v values. Thus, the relative interplay of such factors corresponds to a genuine "structure" effect on the partial cross section behavior. The present study, which uses very accurate PECs and dipole functions, indicates that the final LiH states are formed prevalently in vibrationally excited states with $v = 18$ and 19 rather than in one of the low-lying vibrational target states. It is interesting to note that a similar result was surmised by the earlier model calculations of Kheronskii & Lipovka (1993) who, however, found that the most probable final states corresponded to $v = 15$, 16, and 17.

It is also informative to see the specific dependence of the partial cross sections on the vibrational level of the molecule formed. This is shown by the top plot in Figure 2, where the value of the computed $\sigma_v(E)$ is shown at the energy E_{p1} of the first resonance peaks for each cross section. Thus, we see even more clearly that the largest partial cross section occurs for the $v = 18$ molecular state of LiH. This is an interesting result, since it suggests that radi-

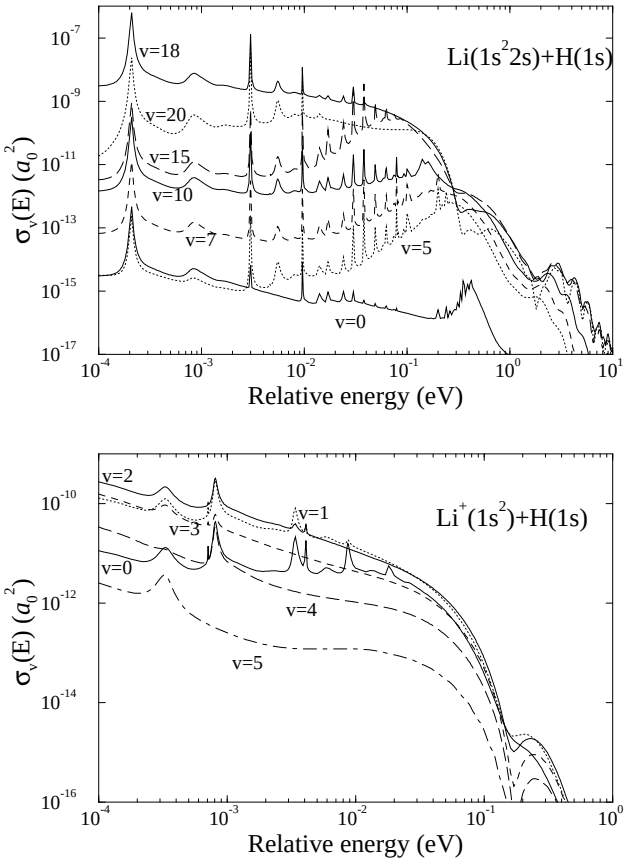

FIG. 1.—Computed partial recombination cross sections as a function of relative collision energy and for several final vibrational levels. (*Top*) Two-body adiabatic processes for the Li($1s^2 2s$) + H($1s$) system; (*bottom*) same set of cross sections for the $Li^+(1s^2)$ + H($1s$) asymptotic partners.

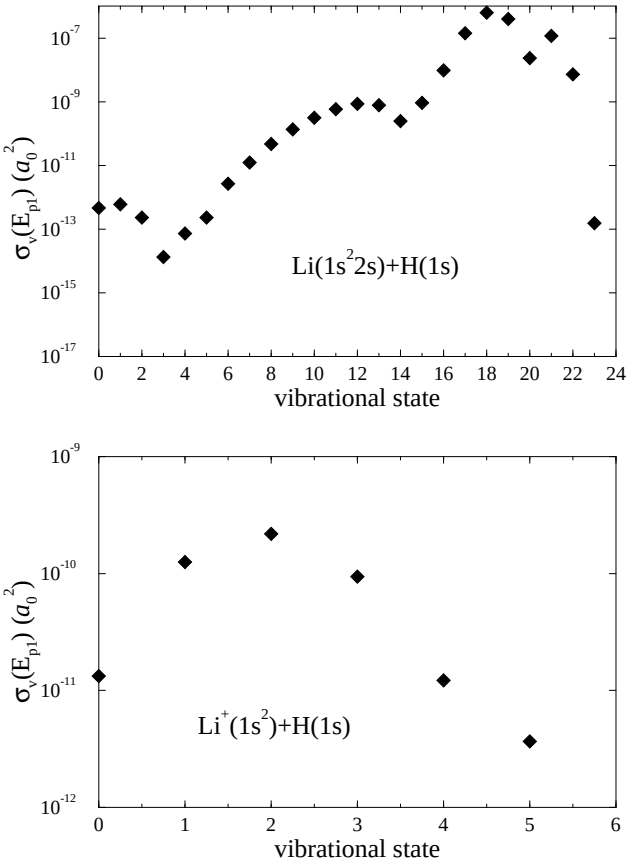

FIG. 2.—Partial recombination cross sections as a function of final vibrational level of the bound molecule. (*Top*) Behavior for the LiH product and (*bottom*) for the LiH^+ product. The energies are those of the lowest appearing resonance position.

ative recombination processes give raise to vibrationally excited products that can, in turn, be detected by successive spontaneous emission of rotovibrational photons as they decay to the lower levels of the bound system.

As mentioned above, several resonant peaks are shown by the computed partial cross sections. In this particular process they are simply the results of "shape" resonances due to the presence of some pseudobound states in the continuum that are trapped by a specific centrifugal barrier, associated to the total angular momentum J of the colliding partners. Because of the limits in the J summation set by $\bar{J}'(v)$, each final vibrational state can show only resonances due to J values up to $\bar{J}' + 1$. Hence, as v increases, the number of resonant pseudobound states in the continuum decreases, and fewer resonances appear for the more vibrationally excited final molecular states. It is interesting to see, however, how the indicative results of Figure 1 show specific features because of some of the resonances being of greater importance than other resonant trapping contributions.

One sees, for instance, that the strongest resonance in the low-energy region appears in all the partial cross sections and is essentially always located at the same collision energy, since the combination of the final v value and of the allowed J controls the labeling of the resonances, but their position is only controlled by the initial angular momentum value. As an example of the labeling that one can carry out to study such resonances (Gianturco, Patriarca, & Roncero 1989), we report in Figure 3 (*top*) the positions and the J values of the resonances for the PEC of the present system. The corresponding partial cross sections for $v = 18$ are also shown to indicate how clearly the lower J values allow one to assign the resonances to specific barrier values. On the other hand, as the energy increases and the corresponding J values increase, spectral congestion in the energy position is reflected by the unresolved, broader resonance peaks shown by the dynamical calculations at the higher collision energies. Thus, the strongest resonance peak that appears in all the partial cross sections at low collision energies (2.1×10^{-4} eV) is shown to be due to the orbiting of the two partners trapped behind the $J = 4$ and $J = 9$ rotational angular momentum barriers.

The total cross section that corresponds to the sum of equation (12) is shown in Figure 4 (*top curve*). The range of collision energies is the same one examined above. As expected, the overall shape and energy dependence is dominated by the $\sigma_v(E)$ for $v = 18$, which is the largest of all the contributing partial cross sections, as already discussed above. On the whole, the calculated cross sections vary over about 8 orders of magnitude when going from about 10^{-4} eV up to about 10 eV of collision energy. They markedly decrease at higher energies because of the marked reduction of the interaction time with respect to the time needed to emit the radiation. Our present results are in very good agreement with those published recently by Dalgarno et al. (1996), in which they used a different potential energy curve (Partridge & Langhoff 1981) that supports one bound level less than the one we employed here (Berriche 1995), which has $v = 23$ as its highest vibrational bound state. As a consequence, the strong peak shown at low energies by our calculations is more than 1 order of magnitude larger than the one shown by Dalgarno et al. (1996), since the latter lacks the contribution from the $J = 4$, $v = 23$ resonance at that energy. On the whole, however, the two curves are very similar to each other and turn out to produce very similar association rates.

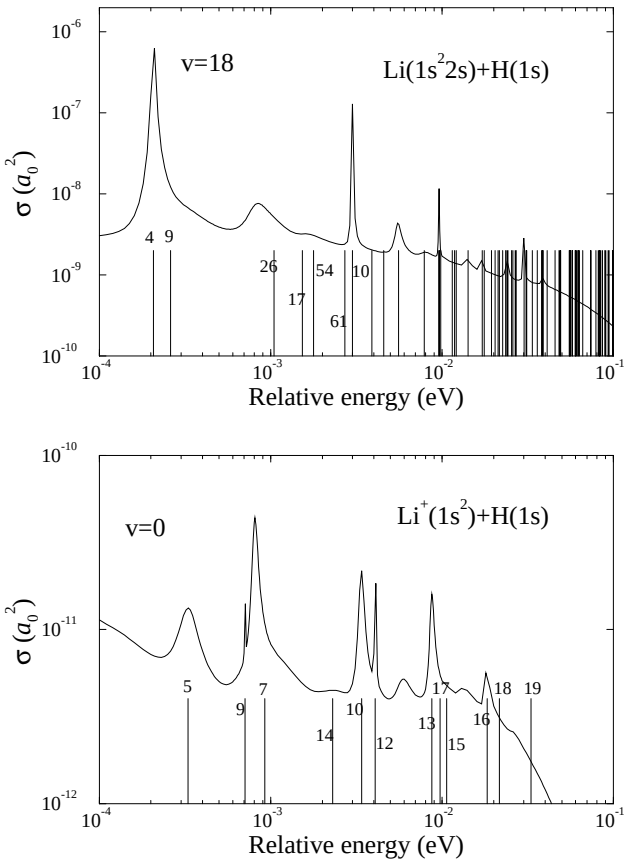

FIG. 3.—Sequence of shape resonances, in the low-energy region of relative collisions, as a function of the angular momentum value for the effective potential. (*Top*) Situation for the LiH system for which the $\sigma_{v=18}$ curve is also shown; (*bottom*) situation for the $Li^+ + H$ system for which the $\sigma_{v=0}$ is also shown.

The last quantity, computed by numerical quadrature from equation (8), is shown in more detail in Table 1, in which the present computed values (in units of $cm^3\ s^{-1}$) are reported for temperatures ranging from $T = 50$ K up to

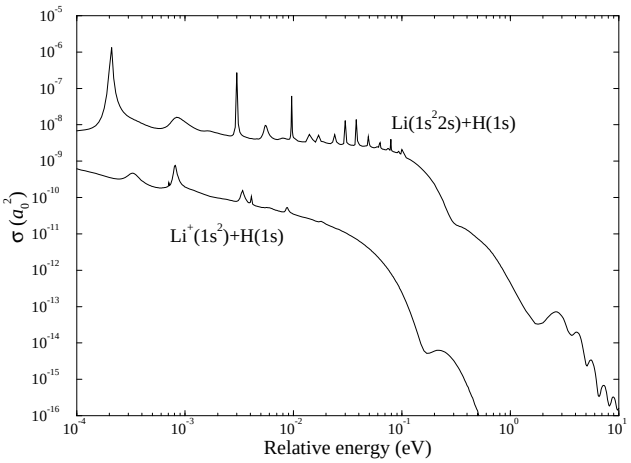

FIG. 4.—Total radiative association cross sections as a function of collision energy: (*top curve*) The LiH molecular product; (*bottom curve*) the LiH^+ molecular product.

TABLE 1

COMPUTED RECOMBINATION RATES FOR THE Li($1s^2 2s$) + H(1s) REACTION

T (K)	Present Results	Dalgarno et al. (1996)
50	2.36×10^{-20}	3.00×10^{-20}
80	2.32×10^{-20}	3.12×10^{-20}
100	2.34×10^{-20}	3.17×10^{-20}
150	2.41×10^{-20}	3.26×10^{-20}
200	2.46×10^{-20}	3.29×10^{-20}
300	2.47×10^{-20}	3.25×10^{-20}
400	2.40×10^{-20}	3.11×10^{-20}
500	2.28×10^{-20}	2.94×10^{-20}
600	2.15×10^{-20}	2.75×10^{-20}
700	2.02×10^{-20}	2.57×10^{-20}
800	1.89×10^{-20}	2.39×10^{-20}
900	1.77×10^{-20}	2.23×10^{-20}
1000	1.66×10^{-20}	2.08×10^{-20}
1200	1.46×10^{-20}	1.82×10^{-20}
1500	1.22×10^{-20}	1.51×10^{-20}
2000	9.35×10^{-21}	1.15×10^{-20}
2500	7.45×10^{-21}	9.11×10^{-21}
3000	6.1×10^{-21}	7.4×10^{-21}
3500	5.1×10^{-21}	6.2×10^{-21}
4000	4.4×10^{-21}	5.3×10^{-21}
4500	3.8×10^{-21}	4.6×10^{-21}
5000	3.3×10^{-21}	4.0×10^{-21}

NOTE.—Computed recombination rates (units of cm^3 s^{-1}) for the Li($1s^2 2s$) + H(1s) reaction. The present results are compared with those from Dalgarno et al. 1996.

$T = 5000$ K and are compared with the previous results from Dalgarno et al. (1996). One clearly sees there that both calculations are indeed very close to each other and span the same range of orders of magnitude: our calculations are constantly smaller than those from Dalgarno et al. (1996) by about 20%, while both are much smaller than the earlier estimates by Kheronskii & Lipovka (1993), which turned out to be between 3 and 4 orders of magnitude larger than ours.

4. RECOMBINATION PROCESSES FOR LiH IONS

In the case of ionic partners, two possible channels exist for the formation of LiH^+ from radiative recombination collisions, i.e., equations (2b) and (2c). However, equation (2b) refers to the formation of the ionic molecule in its ground electronic state, while equation (2c) corresponds asymptotically to an excited state of the final products. Thus, the formation of LiH^+ in its ground state comes from asymptotic partners such as $Li^+(1s^2)$ and H(1s), which follow the BO PEC corresponding to the $X^2\Sigma^+$ symmetry. Since this is the only possible state that one can consider, the corresponding multiplicity p in equation (6) is equal to 1.

4.1. *Ionic Recombination via the $X\,^2\Sigma^+$ Potential*

The currently computed partial cross sections, $\sigma_v(E)$, are shown in the lower part of Figure 1 for all the possible final states, much fewer than for the neutral system, since the shallower potential well of LiH^+ ($X\,^2\Sigma^+$) only supports bound levels up to $v = 5$. The same range of energy values have been considered in this case as for the neutral system.

The general structure of the partial cross sections and their general dependence on the collision energy is similar to the one found before: the partial contributions initially increase in magnitude as v increases but rapidly reach their maximum values for $v = 2$, then decreasing monotonically until $v = 5$. The size variation as a function of v for the lowest resonance position (at $E_{p1} = 3.3 \times 10^{-4}$ eV) is shown in Figure 2 (*bottom*) for all the partial contributions: they span a smaller range of orders of magnitude than that for the neutral molecule. Furthermore, the largest values of σ_v are in this case up to 3 orders of magnitude smaller than those for the neutral molecule formation. In this case, in fact, the much smaller number of final bound states and the smaller values of the dipole moment involved (Gianturco et al. 1996) over a similar range of relative distances qualitatively explain this size reduction.

As in the previous system, however, a sizable number of shape resonances are shown by the partial cross sections, as one clearly sees from the curves of Figure 1. However, they are much fewer and rapidly disappear as the collision energy increases. This is also shown by their actual labeling by J values shown in Figure 3 (*bottom*), where the actual curve for the $\sigma_v(E)$ for $v = 0$ is also shown for comparison. As the final states of bound diatomics are much fewer, the corresponding sequence of resonances does not show spectral congestion as for the LiH products; therefore, the nearly all isolated shape resonances could be clearly assigned to specific J values across the energy range. For highest the J values, on the other hand, the increase of σ_v with respect to the background cross section contribution is rather negligible. This could be expected because of the fact that only the lower σ_v values have contributions from the shape resonances, since higher v values are supported only by a smaller range of J values.

Such an effect is clearly seen by the results for the total cross sections, the sum of equation (7), which are shown in Figure 4 (*bottom curve*). The radiative recombination cross sections into the ground electronic state of the ionic molecule are here markedly smaller than those pertaining to the neutral species, reported in the same figure: the effects of the specific resonant region is also less marked, and, as the relative energy increases, they become very rapidly less important than the corresponding process between neutral partners. From 10 meV up to about 100 meV, for instance, the total cross sections of the ion are from 5 to 7 orders of magnitude smaller than those for the neutral molecule. This behavior could be easily understood if one considers the differences between PECs of the two processes: the potential well is much shallower in the case of LiH^+, and the equilibrium geometry (R_{min}) is further out at $4.15a_0$ (for LiH is at 3.011 a_0). This means that a much smaller range of impact parameters (angular momentum values) is relevant for the recombination process, since their larger values involve only effective potentials that are monotonically repulsive and therefore do not support any bound state. Futhermore, the angular momentum operator is also smaller over the region of radial variation corresponding to ionic bound states (Berriche 1995; Berriche & Gadea 1995).

To our knowledge, no other data for calculated partial cross sections are available from the literature, while the total cross sections were also computed recently by Dalgarno et al. (1996). Their results are very close to ours, and the present curve in the Figure 4 (*bottom*) is indeed very similar in shape and value to that shown by those authors. This is very reassuring since the two calculations employed different potential energy curves and used entirely different computational codes. That they are indeed producing essentially the same results could be seen by the behavior of the corresponding rates, obtained here by integration of

equation (8), evaluated over a range of temperatures from 5 K up to 5000 K. The two sets of results are reported in Table 2 and clearly show that the two calculations generate practically the same rate values, with the present results being, on average, about 10% larger than those from Dalgarno et al. (1996).

4.2. *Ionic Recombination with the* $2\,^2\Sigma^+$ *Potential*

In the case of ionic partners, as mentioned before, the difference between the ionization potential of hydrogen and lithium (8.214 eV) causes the possibility of two different asymptotic states of the ionic bound species. In the previous subsection, we have examined the ground electronic state that separates into the $Li^+(1s^2)$ and H(1*s*) atomic partners, while the other option is to consider the system that follows the electronically excited PEC ($2\,^2\Sigma^+$) and separates into $Li(1s^2 2s)$ and H^+. In this case, however, the process of radiative recombination occurs by emission of a photon from the excited initial electronic state that drives the collision into the final, ground electronic state of the bound ionic molecule. The two PECs involved were taken from our previous calculations (Berriche 1995; Gianturco et al. 1996), while the transition moment is the same as the one given by Dalgarno et al. (1996). Since the PEC involved turned out to be very similar to those used earlier (Dalgarno et al. 1996), the corresponding transition moment values are presumably also well described by their estimates.

The partial cross sections for each of the final vibrational states into which the ionic molecule can be formed were computed using the procedure discussed above, and the results are displayed in the Figure 5 (*top*) over the usual range of collision energies. It is interesting to note right away that the partial cross sections are between 5 and 6 orders of magnitude larger than those computed before for the ground electronic state. This difference could be understood by considering that, even if all other elements remain

TABLE 2

COMPUTED RECOMBINATION RATES FOR THE $Li^+(1s^2)$ + H(1s) ADIABATIC REACTION

T (K)	Present Results	Dalgarno et al. (1996)
50	1.79×10^{-22}	1.62×10^{-22}
80	1.57×10^{-22}	1.43×10^{-22}
100	1.46×10^{-22}	1.33×10^{-22}
150	1.23×10^{-22}	1.13×10^{-22}
200	1.06×10^{-22}	9.76×10^{-23}
300	8.13×10^{-23}	7.53×10^{-23}
400	6.48×10^{-23}	6.01×10^{-23}
500	5.31×10^{-23}	4.94×10^{-23}
600	4.45×10^{-23}	4.14×10^{-23}
700	3.79×10^{-23}	3.54×10^{-23}
800	3.29×10^{-23}	3.07×10^{-23}
900	2.88×10^{-23}	2.69×10^{-23}
1000.....	2.55×10^{-23}	2.39×10^{-23}
1200.....	2.06×10^{-23}	1.93×10^{-23}
1500.....	1.56×10^{-23}	1.46×10^{-23}
2000.....	1.08×10^{-23}	1.01×10^{-23}
2500.....	8.03×10^{-24}	7.55×10^{-24}
3000.....	6.3×10^{-24}	5.9×10^{-24}
3500.....	5.1×10^{-24}	4.8×10^{-24}
4000.....	4.2×10^{-24}	4.0×10^{-24}
4500.....	3.6×10^{-24}	3.4×10^{-24}
5000.....	3.1×10^{-24}	2.9×10^{-24}

NOTE.—Computed recombination rates for the $Li^+(1s^2)$ + H(1*s*) adiabatic reaction (units of $cm^3\ s^{-1}$). The present results are compared with those from Dalgarno et al. 1996.

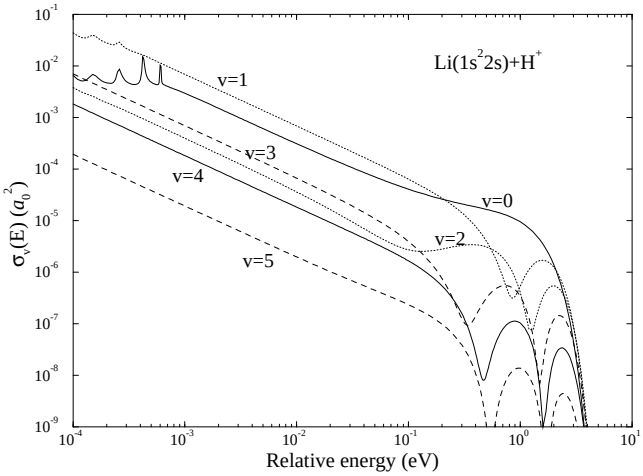

FIG. 5.—Partial recombination cross sections for all possible final vibrational states of the product as a function of collision energy. The process considered is the nonadiabatic ($2\,^2\Sigma^+ \rightarrow X\,^2\Sigma^+$) transition to the LiH^+ final product.

equal, the frequencies of the emitted photons are at least 3 orders of magnitude larger for the electronic transitions and play an important role in equation (6). Furthermore, the transition moment itself is larger than in the case in which only one BO potential is involved in its calculation.

The dependence of the $\sigma_v(E)$ values on the final vibrational level of the bound state is also different from that shown before by the systems formed via only one PEC: here the $v = 1$ ionic molecule is the most likely product over 4 orders of magnitude of collision energy and becomes smaller than the probability of forming LiH^+ in the $v = 0$ state only above a collision energy of about 0.3 eV. The final products formed into the $v = 3$ and $v = 2$ vibrational states also show a similar behavior and at nearly the same collision energy. The reason should be related to the behavior of the transition moment (Dalgarno et al. 1996), which we have reported for clarity in Figure 6 for both ionic target formations. One sees that the above quantity shows a marked negative maximum around $5a_0$ and then decreases constantly as R increases. As a result, radiative transitions into the lowest vibrational states involve larger transition moment values and become favored by the Franck-Condon principle.

The results shown in Figure 5 indicate, as for the systems analyzed before, the presence of marked resonances, especially in the low-energy regime. In this instance the presence of open channel resonances is due to the temporary trapping of the colliding partners by the effective potential from the initial, excited electronic state. The actual PEC supports in our case 27 bound levels, but larger $\bar{J}(v)$ values are able here to perform the trapping of continuum states that can give rise to resonances. This is related to the additional role of the transition moment, which decreases at low R values, hence favoring transitions from more "extended" pseudobound states into the lower lying vibrational levels of the ionic molecule. On the other hand, the partial cross sections produced by the lower PEC of the ion (Figs. 2 and 3) indicate a dominance of vibrationally excited final states because of the different shape of the dipole moment involved.

The different behavior of the relevant transition moment is also reflected on the labeling of the resonances, as one can

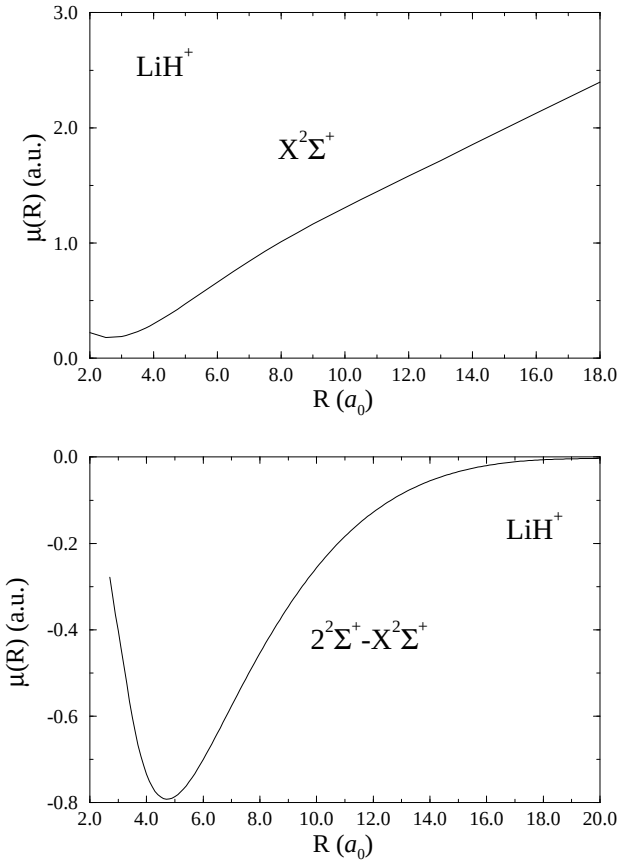

FIG. 6.—General behavior of transition dipole moments for the LiH^+ system. (*Top*) Dependence of $\mu(R)$ on internuclear distance for the $X\,^2\Sigma^+$ electronic state (from Voitik et al. 1990). (*Bottom*) Same behavior for the nonadiabatic transition dipole moment for the $2\,^2\Sigma^+ \rightarrow X\,^2\Sigma^+$ de-excitation process (from Dalgarno et al. 1996).

see in the example shown in Figure 7 (*inset*). What we report there is the location of the lower lying resonances for each of the relevant angular momentum values and the comparison with the $v = 0$ partial cross section behavior. One sees that, since $\bar{J}(v = 0) = 16$, one finds resonances up to

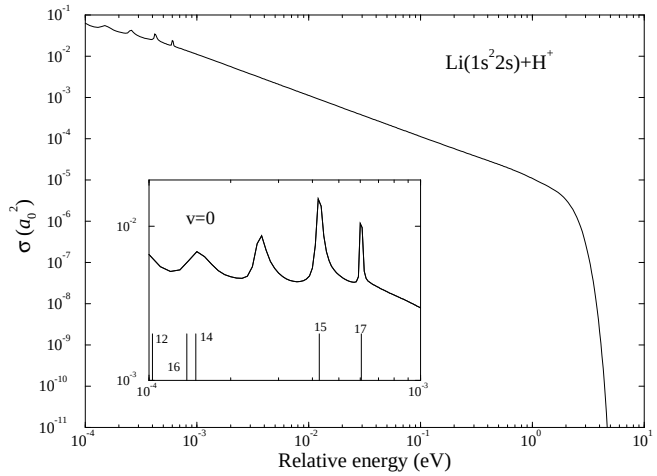

FIG. 7.—Total radiative recombination cross section as a function of collision energy for the LiH^+ final bound products formed via nonadiabatic transitions from the continuum of $Li(1s^22s) + H^+$. (*Inset*) Labeling of the shape resonances of the σ_v cross sections for $v = 0$ in the same process.

TABLE 3

COMPUTED RADIATIVE RECOMBINATION RATES FOR THE NONADIABATIC PROCESS ($2\,^2\Sigma^+ \rightarrow X\,^2\Sigma^+$) FOR THE $Li(1s^22s) + H^+$ PARTNERS

T (K)	Present Results	Dalgarno et al. (1996)
50	7.66×10^{-15}	7.66×10^{-15}
80	6.14×10^{-15}	6.15×10^{-15}
100	5.52×10^{-15}	5.53×10^{-15}
150	4.54×10^{-15}	4.55×10^{-15}
200	3.95×10^{-15}	3.96×10^{-15}
300	3.24×10^{-15}	3.25×10^{-15}
400	2.81×10^{-15}	2.82×10^{-15}
500	2.52×10^{-15}	2.53×10^{-15}
600	2.31×10^{-15}	2.32×10^{-15}
700	2.14×10^{-15}	2.14×10^{-15}
800	2.00×10^{-15}	2.01×10^{-15}
900	1.89×10^{-15}	1.90×10^{-15}
1000.....	1.80×10^{-15}	1.81×10^{-15}
1200.....	1.65×10^{-15}	1.65×10^{-15}
1500.....	1.48×10^{-15}	1.48×10^{-15}
2000.....	1.29×10^{-15}	1.29×10^{-15}
2500.....	1.15×10^{-15}	1.16×10^{-15}
3000.....	1.1×10^{-15}	1.1×10^{-15}
3500.....	9.7×10^{-16}	9.8×10^{-16}
4000.....	9.1×10^{-16}	9.1×10^{-16}
4500.....	8.5×10^{-16}	8.6×10^{-16}
5000.....	8.1×10^{-16}	8.1×10^{-16}

NOTE.—Computed radiative recombination rates for the nonadiabatic process ($2\,^2\Sigma^+ \rightarrow X\,^2\Sigma^+$) for the $Li(1s^22s) + H^+$ partners. The present results (units of $cm^3\ s^{-1}$) are compared with those produced by Dalgarno et al. 1996.

$J = 17$. However, one of the resonant shapes appearing in the cross sections cannot be assigned to a specific J value and may be due to an enhancement effect from the shape of the transition moment.

The total summed cross sections are reported in Figure 7 (*top*) and turn out to be much larger than any of the previous systems: recombination from an excited electronic state is therefore, if the state is available, occurring with a much larger probability than the recombination from one single BO PEC of the system, either neutral or ionic. Our results are again very similar to those given by Dalgarno et al. (1996), as one can clearly see from the final recombination rates reported in Table 3 over the same range of temperatures discussed earlier for the other electronic PECs. Our results are essentially coincident with the ones given by those authors, indicating that the minor differences in the PECs for the excited state are essentially canceled by having used the same values for the transition moment.

5. CONCLUSIONS

In the previous sections we have carried out quantum mechanical calculations of the radiative association rates for the molecules of LiH and LiH^+ over a broad range of temperatures. The main results of the above work are the following:

1. The association rates for the formation of the two molecules are found to be much smaller than those previously suggested (Lepp & Shull 1984; Kheronskii & Lipovka 1993) but turn out to be in very good agreement with the more recent quantum calculations on the same systems (Dalgarno et al. 1996).

2. The formation of ionic molecules can proceed via two different pathways, i.e., either adiabatically along a single

PEC for the ionic ground electronic state ($X\,^2\Sigma^+$) or nonadiabatically by reaching the ground state through an electronic transition from the charge-exchange excited state, $2\,^2\Sigma^+$. In the latter instance the rates of formation are found to be much larger, and the corresponding process exhibits a much higher probability of occurring than the two-body recombination reactions, which proceed via adiabatic pathways.

3. All the processes considered indicate at low energies the marked effects of resonant reactions, i.e., of barrier trapping of the colliding partners before the recombination reaction. Such dynamical lengthening of the interaction times has important consequences on the corresponding values of the integrals in equation (6), since the continuum resonant functions show much larger values in the region of relative distances in which the bound functions are the largest.

One of the main consequences of the present results for the lithium chemistry in the primordial medium is that the expected abundance of the LiH molecule gets reduced by at least 2 orders of magnitude (Stancil, Lepp, & Dalgarno 1996) with respect to the earlier estimates (Lepp & Shull 1984; Puy et al. 1993). Hence, the LiH abundance comes closer to the limit of about 3×10^{-12} [H], which corresponds to a negligible attenuation of primary cosmic background radiation anisotropies (Maoli, Melchiorri, & Tosti 1994). Furthermore, Stancil et al. (1996) estimate that the expected abundance is further reduced, possibly down to about 10^{-17} [H], by the additional effects from the exothermic reaction,

$$\mathrm{LiH} + \mathrm{H} \rightarrow \mathrm{Li} + \mathrm{H}_2 \,, \qquad (13)$$

about which, however, very little is known and only qualitative estimates exist today.

In conclusion, the present ab initio calculations have strived to treat all aspects of the adiabatic radiative recombination reaction on the same footing. Thus, the relevant PECs have been taken from accurate quantum chemistry calculations, the corresponding transitions have also been obtained as accurately as possible, and the continuum functions have been computed by solving correctly the numerical scattering equations for a broad range of relative energies and for all allowed impact parameters. Finally, the corresponding rates have been obtained by numerically stable quadratures over a very large set of fixed-energy results for all systems considered. The fact that the present findings turn out to be in close agreement with those recently published by other authors (Dalgarno et al. 1996) certainly supports the good reliability of the current results and the likelihood that the reactive channels need to be considered if the presence of LiH has to play a role for the observation of primordial clouds (Maoli et al. 1996).

The formation of the ionic species, on the other hand, is strongly helped by the presence of an additional channel, whereby the reaction can proceed nonadiabatically via two different PECs. The preferential channel for LiH^+ formation, however, is the one in which the asymptotic partners to the involved adiabatic state contain, as an ion, the atom with the higher ionization potential that tends to recombine first (Stancil et al. 1996). Thus, we find again that the ion recombination is preferentially proceeding along the $X\,^2\Sigma^+$ electronic curve rather than along the $2\,^2\Sigma^+$ one, which is followed during the recombination of ionized hydrogen.

Another interesting aspect of the present study is that nearly all processes considered proceed to the formation of LiH and LiH^+ molecules, which are preferentially vibrationally excited and which could therefore further radiate spontaneously in the IR region and after 10^{-2}–10^{-3} s. If one combines this piece of information with our earlier findings (Gianturco et al. 1996) about preferential bound-bound radiative transitions between rotovibrationally excited levels of LiH and LiH^+, one can see that radiative processes preferentially involve transitions into bound states that are above the ground vibrational level of the molecules; therefore, the question of accurate abundance estimates becomes crucial to the possible observational detection of further spontaneous emissions from excited molecular bound states.

The financial support of the Italian National Research Council (CNR) and the Italian Ministry of University and of Scientific Research (MURST) are gratefully acknowledged. The initial help of H. Berriche and F. X. Gadea is also thanked, as well as many helpful discussion with A. Dalgarno and P. C. Stancil during F. A. G.'s visit to the Harvard ITAMP Center in the summer of 1995. Finally, the helpful support and encouragement of F. Melchiorri and his research group are also warmly acknowledged.

REFERENCES

Babb, J. F., & Dalgarno, A. 1995, Phys. Rev. A, 51, 3021
Berriche, H. 1995, Thèse d'État, Université Paul Sabatier, Toulouse, France
Berriche, H., & Gadea, F. X. 1995, Chem. Phys. 191, 119
Dalgarno, A., Kirby, K., & Stancil, P. C. 1996, ApJ, 458, 397
Dalgarno, A., & Lepp, S. 1987, in Astrochemistry, ed. S. Tarafdar & M. P. Varshni (Dordrecht: Reidel), 109
Gianturco, F. A., Gori Giorgi, P., Berriche, H., & Gadea, F. X. 1996, A&AS, 117, 1
Gianturco, F. A., Patriarca, M., & Roncero, O. 1989, Mol. Phys., 67, 281
Herzberg, G. 1950, Spectra of Diatomic Molecules (New York: Van Nostrand)
Kheronskii, V. K., & Lipovka, A. A. 1993, Astrofiz. Issled., 36, 88
Lepp, S., & Shull, J. M. 1984, ApJ, 280, 465
Maoli, R., Ferrucci, V., Melchiorri, F., Signore, M., & Tosti, D. 1996, ApJ, 457, 1
Maoli, R., Melchiorri, F., & Tosti, D. 1994, ApJ, 425, 372
Partridge, H., & Langhoff, S. R. 1981, J. Chem. Phys., 74, 2361
Puy, D., Alecian, G., Le Bourlot, J., Léorat, J., & Pineau de Fôrets, G. 1993, A&A, 267, 337
Schadee, A. 1978, J. Quant. Spectrosc. Radiat. Transfer, 19, 451
Silk, J. 1983, MNRAS, 205, 705
Smith, K. 1971, The Calculation of Atomic Collision Processes (New York: Wiley)
Stancil, P. C., Lepp, S., & Dalgarno, A. 1996, ApJ, 458, 401
Voitik, J., Cespiva, L., Savrda, J., & Paidarova, I. 1990, J. Mol. Spectrosc., 142, 279
Zygelman, B., & Dalgarno, A. 1990, ApJ, 365, 239